

# Investigation of Solvothermal Synthesis and Formation Mechanism of Fe<sub>2</sub>O<sub>3</sub>/C Microspheres

H. Safarzadeh, R. Ebrahimi-Kahrizangi, M. Ghaderi\*, A. Saffar-Talouri

*Young Researchers and Elite Club, Najaf Abad Branch, Islamic Azad University, Najaf Abad, Iran*

\*e-mail: [mo.ghaderi@yahoo.com](mailto:mo.ghaderi@yahoo.com)

In this research we report a one-step method to fabricate Fe<sub>2</sub>O<sub>3</sub>/C microspheres by using the rolling scales oxides via the solvothermal approach. The thermal gravimetric Analysis (TGA) experiment was carried out in order to determine the amount of carbon in the synthesized samples. Only Fe<sub>2</sub>O<sub>3</sub> peaks could be observed from X-ray diffractometry patterns; the carbon in the composite was amorphous. The content of the carbon in the composite was calculated to be about 72 wt.%. After annealing at 800°C, scanning electron microscopy images showed that the surface of microspheres was rather smooth and their diameters were in the range of 1–3.5 μm. The investigation of Fe<sub>2</sub>O<sub>3</sub>/C microspheres formation mechanism revealed that Fe<sub>2</sub>O<sub>3</sub> nanoparticles are homogeneously distributed in the carbon matrix.

*Keywords: microsphere, solvothermal approach, Fe<sub>2</sub>O<sub>3</sub>, carbon, electrode.*

УДК 662.7

## 1. INTRODUCTION

Nanostructured transition metal oxides have received great interest as electrodes for lithium-ion batteries [1]. Among these, Fe<sub>2</sub>O<sub>3</sub> is an *n*-type, eco-friendly semiconductor that can be used in household and industrial applications for detection of toxic vapors and harmful and flammable gases. This is why, Fe<sub>2</sub>O<sub>3</sub> microspheres with a hollow structure are used to make acetone and CO sensors [2]. Also, Fe<sub>2</sub>O<sub>3</sub> microspheres are widely used in fabrication of the DNA electrochemical biosensors for determining nucleic acid sequences [3]. The electrodes made of nanooxides of transition metals have a significantly high electrochemical capacity of 700 mAh·g<sup>-1</sup>. Indeed, they can be regarded as promising substitutes for carbon electrodes and Ni-metal hydride in Li-ion batteries [4]. However, the most critical problem that hinders the commercial use is their large specific volume change, resulting in the aggregation of small particles into larger ones [5]. A continuous volume change during charge-discharge results in disintegration of the electrode materials and capacity fading upon cycling [6]. To overcome the volume changes is possible through the use of nano-sized materials and formation of micro composites with carbon, in which the oxide nanoparticles are embedded within the composite. The carbon can act as a barrier to suppress the aggregation of active nano particles and thus increase their structural stability during cycling [7]. The carbon has a high electronic conductivity, and it can improve the conductance of the active materials and the electrochemical capacity of nanooxides.

In order to produce microcomposites of metal oxides with carbon, several methods, including molten salt process [8], two-step synthesis by graphene

[9], hydroxide and hydrothermal routes [10], flocculation [11], sol-gel [12], and spray pyrolysis [13], have been suggested.

The present research aims at using the rolling scales oxide wastes that have not found much application so far in a one-step production of Fe<sub>2</sub>O<sub>3</sub>/C composite microspheres by the solvothermal method.

## 2. MATERIALS AND METHODOLOGY

The most important materials used in this research were: 2.5 g of oxide shells with 97 wt% iron oxide purity, 160 ml ethanol (96%), 50 ml Sulfuric acid 99%, 2 g glucose 100%, 5 ml nitric acid 65%, and 2 g sodium hydroxide.

First, oxide shells were dissolved in a concentrated sulfuric acid. Then the solution was exposed to severe magnetic stirring at 100°C for 30 min. Following that, nitric acid was slowly added to the solution. This resulted in a complete solution of all oxide solid particles. Then the solution was heated until it was entirely dried. The white precipitate at the bottom largely contained Fe<sup>+3</sup> [14].

Next, 2.5 g of Fe<sup>+3</sup> were mixed with 160 ml of ethanol and thoroughly stirred with a magnetic stirrer. The solution was heated up to 60°C until all the iron salt was solved. Due to the solving of the iron salt, the solution pH decreased to 1.7. In the next stage, 2 g of glucose were solved in 5 ml deionized water and then added to the above solution. The solution was transferred to an autoclave and stored at 185°C for 25 h and then air-cooled to room temperature. The resulting black precipitates were washed several times with ethanol and centrifuged. This caused the separation of all anions and cations from the precipitates. The as-prepared precipitates were

designated amorphous  $\text{Fe}_2\text{O}_3/\text{C}$  hybrid microspheres. The products were finally dried in an oven at  $50^\circ\text{C}$  for 10 h.

The amorphous  $\text{Fe}_2\text{O}_3/\text{C}$  samples obtained via the solvothermal reaction were annealed in the tube furnace at  $800^\circ\text{C}$  in an Argon-rich atmosphere.

The composite properties such as crystallite or amorphous structure, crystallinity degree, and grain size were investigated by a Philips X'pert high score X-ray diffractometer with  $\text{Cu K}_\alpha$  radiation ( $2\theta$  is chosen in the range of  $10\text{--}90^\circ$ ). Thermogravimetric analysis was performed on a TGA 401 instrument at up to  $800^\circ\text{C}$  and the heating rate of  $10^\circ\text{C min}^{-1}$  in air. The microstructure of the as-prepared composite was observed with the scanning electron microscope (LEO-VP435).

### 3. RESULTS AND DISCUSSION

#### 3.1. Characterization of $\text{Fe}_2\text{O}_3/\text{C}$ microspheres

Figure 1 shows X-ray diffraction (XRD) patterns of amorphous and annealed  $\text{Fe}_2\text{O}_3/\text{C}$  microspheres. As can be seen in Fig. 1a,  $\text{Fe}_2\text{O}_3/\text{C}$  microspheres are amorphous. Heating in argon atmosphere at  $800^\circ\text{C}$  caused significant crystallization of  $\text{Fe}_2\text{O}_3/\text{C}$  samples (Fig. 1b). The peaks of the annealed sample are located in  $33.2$ ,  $35.7$ ,  $40.8$ ,  $54.2$ ,  $62.4$ , and  $64.2$  angles which are assigned as (104), (110), (113), (024), (116), (214), and (300) reflections, respectively. The carbon is amorphous in both conditions which is similar to the results reported by Qiao [15]. The intensity of some peaks is weak due to the presence of impurities in the composite. Also, during the annealing process some amount of  $\text{Fe}_2\text{O}_3$  changed into  $\text{Fe}_3\text{O}_4$  because of a high temperature and the carbon presence. The  $\text{Fe}_2\text{O}_3$  grain size was calculated based on the modified Debye Scherrer's equation (eq. 1):

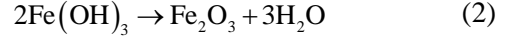
$$L = 0.89\lambda / \beta \cos\theta$$

$$\beta = \frac{k\lambda}{L \cos\theta} \Rightarrow \ln\beta = \ln \frac{k\lambda}{L} + \ln \frac{1}{\cos\theta}. \quad (1)$$

By plotting  $\ln\beta$  variations against  $\ln(1/\cos\theta)$  the intercept of a least squares line regression,  $\ln = K\lambda/L$ , is obtained. After the calculations of the phase analysis (XRD) results of  $\text{Fe}_2\text{O}_3/\text{C}$  powder, the obtained y-intercept was  $-5.4886$ . Since  $A^\circ = 1.54059\lambda$  and  $K = 0.89$ , the  $\text{Fe}_2\text{O}_3$  nanoparticles size ( $L$ ) was averaged calculated as  $30 \pm 4$  nm.

Figure 2 shows the weight variations diagram for amorphous  $\text{Fe}_2\text{O}_3/\text{C}$  powder samples resulting from solvothermal reaction. Thermogravimetric curve shows that the weight loss occurs in three stages. The first stage takes place in the temperature range of  $100$  to  $330^\circ\text{C}$ . The weight loss at this stage is estimated to  $5.8\%$ , which can be due to the evaporation and removal of water from the composite [5].

The second stage happens in the temperature range of  $330$  to  $360^\circ\text{C}$  and the weight loss is calculated to be  $12.2\%$ . The main reason of the weight loss at this stage is that iron hydroxide changes into iron oxide along with the formation of vapor during the process (eqs. 2 and 3).



The third stage, from  $360$  to  $800^\circ\text{C}$ , is related to oxidation of the amorphous carbon. The weight loss in this stage is  $36\%$  [16]. Based on the calculations from thermos-gravimetric curve and complete carbon oxidation, the carbon content in the composite was estimated to be  $72\%$ .

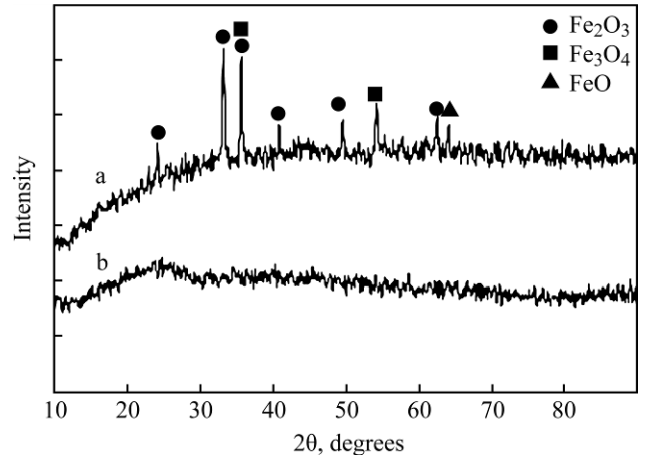


Fig. 1. XRD pattern of  $\text{Fe}_2\text{O}_3/\text{C}$  microspheres in two conditions: (a) without being annealed; (b) annealed.

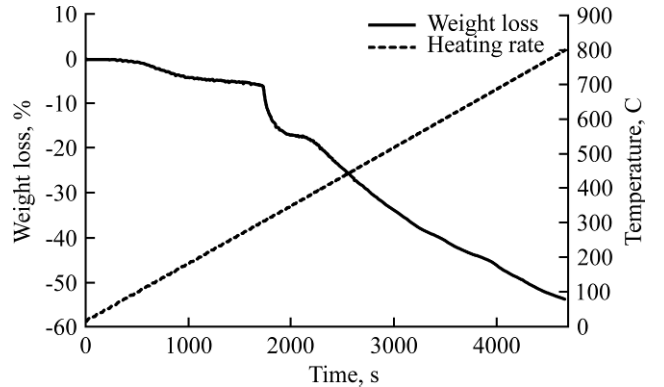
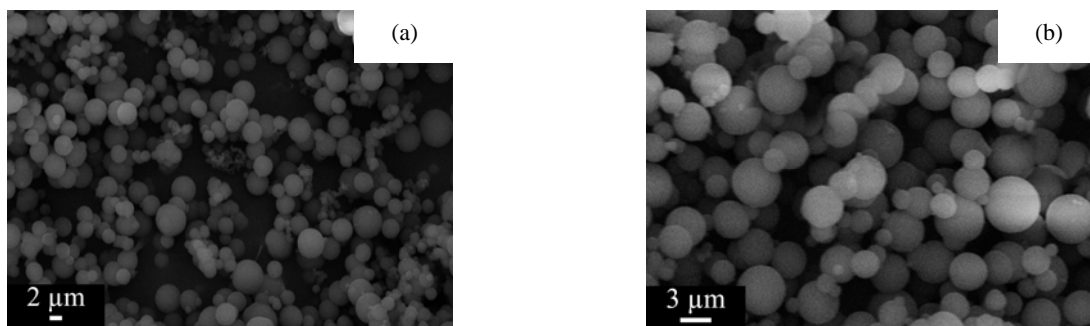


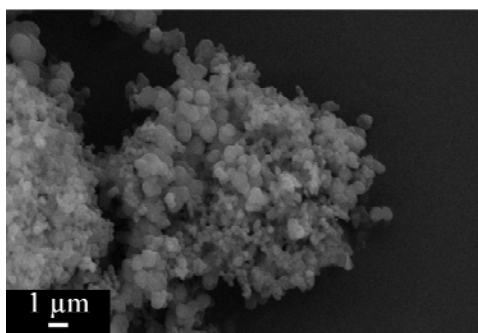
Fig. 2. Thermogravimetric curve of amorphous  $\text{Fe}_2\text{O}_3/\text{C}$  powder samples resulting from solvothermal reaction in the range from room temperature to  $800^\circ\text{C}$ .

Figure 3a shows the spherical morphology of the composites as taken from the surface of  $\text{Fe}_2\text{O}_3/\text{C}$  microspheres. Their sizes are almost uniform and their diameters are in the range  $1\text{--}3.5$   $\mu\text{m}$ . Figure 3b shows the image of  $\text{Fe}_2\text{O}_3/\text{C}$  microspheres with higher magnification after annealing. The size and shape of the microspheres have remained the same after annealing, but the surfaces have become slightly rough due to gas emission. It has been proved that  $\text{Fe}_2\text{O}_3$  nanoparticles are homogeneously distributed in the carbon matrix [5].



**Fig. 3.** SEM image of  $\text{Fe}_2\text{O}_3/\text{C}$  microspheres in which  $\text{Fe}_2\text{O}_3$  nanoparticles ( $30 \pm 4$  nm) are distributed in the carbon spheres: (a) in amorphous condition; (b) annealed at  $800^\circ\text{C}$ .

Results revealed that  $\text{Fe}_2\text{O}_3/\text{C}$  microspheres could not be obtained via the solvothermal treatment below  $140^\circ\text{C}$ , which is in agreement with the reports by other researchers [16]. In the absence of the iron salt precursor no product is obtained from glucose and ethanol. Also, in order to achieve a spherical morphology the solution pH should be less than 2 [16]. Figure 4 shows SEM image of the sample in which the pH value went up to 2.5 because of the addition of adding sodium hydroxide. As can be seen, the morphology tends toward aggregation.



**Fig. 4.** SEM image of a sample with pH = 2.5.

### 3.2. $\text{Fe}_2\text{O}_3/\text{C}$ microspheres formation mechanism

The mechanism of  $\text{Fe}_2\text{O}_3/\text{C}$  microspheres formation comprises two stages, namely nucleation and growth. The initial nucleus shape is inherent and depends on the innate properties of the composite. In contrast, the growth stage is a thermodynamic and controllable factor [17]. The mechanism of formation includes production of aromatic primary compounds containing cations and polymerization of glucose. After that, the carbon and metal oxide nanoparticles are produced simultaneously and metal oxide nanoparticles are distributed in the carbon matrix. In glucose polymerization, hydrophobic groups play the role of tails and include radical combinations of hydrocarbon (C-H). The hydrophilic head includes OH-, CHO-, and COO-groups [16, 18].  $\text{Fe}^{+3}$  cations are attracted by hydrophilic spherical micelle parts due to electrostatic processes [19]. Glucose influences the surface tension of ethanol and can dramatically govern the nucleation rate of  $\text{Fe}_2\text{O}_3$  particles. When the  $\text{Fe}_2\text{O}_3$  nucleation rate

increases, smaller particles with nanometer sizes are formed [19]. Following that, by glucose polymerization, the concentration reaches the critical micelle concentration and a spherical micelle complex, with hydrophobic groups as the micelle core and the hydrophilic hydroxyls as the outer surface of micelle core are formed. Figure 5 shows how  $\text{Fe}_2\text{O}_3/\text{C}$  microspheres are formed. After nucleation, the hydrophilic hydroxyls are still anchored to the closest free molecules [18], which causes the watering of the nucleus and hence the micelle growth.  $\text{Fe}^{+3}$  cations are continuously attracted by the hydrophilic parts of the growing sphere and change into  $\text{Fe}_2\text{O}_3$  after  $\text{Fe}(\text{OH})_3$  is formed. This trend continues until all glucose molecules are consumed.

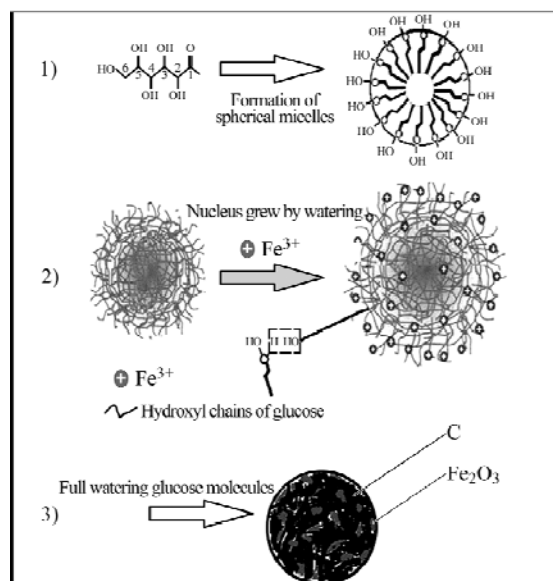


**Fig. 5.** Schematic illustration of formation of initial nuclei of  $\text{Fe}_2\text{O}_3/\text{C}$  microspheres and nucleus growth.

The spherical appearance of the as-synthesized microcomposites can be explained in this way: chemical reactions generally move in a certain direction, which results in the decrease of the Gibbs free energy. Formation of microspheres must be related to the Gibbs free energy. On the other hand, the molecules surface stresses should reach a minimum by formation of spherical morphology, so as to reduce the surface free energy. In fact, in the formation of the final composite shape there is a com-

petition between the surface free energy and the Gibbs free energy. When the particle size is small, the surface free energy is the dominant mechanism and with formation of the spherical morphology reaches a minimum value due to the lowest surface to volume ratio [20].

Gradually, with the increase of the spheres size, the surface free energy plays a less significant role in the material morphology. However, it should be noted that with control of variable such as temperature, precursor concentration, pH, and the like we can make variations as to the role played by either the Gibbs free energy or the surface free energy.

#### 4. CONCLUSIONS

In this research, microspherical Fe<sub>2</sub>O<sub>3</sub>/C composites were prepared via the solvothermal approach by using the mill scale oxide shells and the following results were obtained:

1. XRD patterns quite evidently depicted Fe<sub>2</sub>O<sub>3</sub> peaks. Also, by studying the growth mechanism, it can be inferred that Fe<sub>2</sub>O<sub>3</sub> nanoparticles are homogeneously distributed in the carbon matrix. The carbon content in the composite is amorphous in both annealed and un-annealed conditions.

2. Based on the thermogravimetric curve and complete carbon oxidation, the carbon content in microspherical Fe<sub>2</sub>O<sub>3</sub>/C composites was estimated to be 72%.

3. SEM images revealed a spherical and smooth morphology. The sizes of the microspheres were rather uniform and their diameters were in the range of 1–3.5 μm.

4. For synthesis of Fe<sub>2</sub>O<sub>3</sub>/C microspheres the solution pH should be lower than 2 and the temperature should be above 140°C.

5. In addition to providing carbon, glucose decreases the surface tension of ethanol and increases the nucleation rate of Fe<sub>2</sub>O<sub>3</sub> nanoparticles, thus decreasing the grain size of Fe<sub>2</sub>O<sub>3</sub> particles near the hydrophobic chain.

#### REFERENCES

- Poizot P., Laruelle S., Grugeon S., Dupont L., Tarascon J.M. Towards the Next Generation of Li-ion Batteries Based on Nanomaterials. *Nature*. 2000, vol. 407, 496–499.
- Wang S., Wang T., Yang X., Liu H., Zhang J., Zhu B., Zhang S. Porous α-Fe<sub>2</sub>O<sub>3</sub> Hollow Microspheres and their Application for Acetone Sensor. *J Solid State Chem*. 2000, vol. 183, 2869–2876.
- Zhang W., Yang T., Li X., Wang D., Jiao K. Conductive Architecture of Fe<sub>2</sub>O<sub>3</sub> Microspheres/Self-doped Polyaniline Nanofibers on Carbon Ionic Liquid Electrode for Impedance Sensing of DNA Hybridization. *Biosens Bioelectron*. 2009, vol. 25, 428–434.
- Anandan K., Rajendran V. Morphological and Size Effects of NiO Nanoparticles via Solvothermal Process and their Optical Properties. *Mat Sci Semicon Proc*. 2011, vol. 14, 43–47.
- Qiao H., Luo Q., Fu J., Li J., Kumar D. Solvothermal Preparation and Lithium Storage Properties of Fe<sub>2</sub>O<sub>3</sub>/C Hybrid Microspheres. *J Alloy Compd*. 2012, vol. 513, 220–223.
- Huang X.H., Wang C.B., Zhang S.Y., Zhou F. CuO/C Microspheres as Anode Materials for Lithium Ion Batteries. *Electrochim Acta*. 2011, vol. 56, 6752–6756.
- Qiao H., Yao D., Cai Y., Huang F., Wei Q. One-pot Synthesis and Electrochemical Property of MnO/C Hybrid Microspheres. *Ionics*. 2013, vol. 19, 595–600.
- Hassan M.F., Rahman M.M., Guo Z.P., Chen Z.X., Liu H.K. Solvent-assisted Molten Salt Process: A New Route to Synthesize Fe<sub>2</sub>O<sub>3</sub>/C Nanocomposite and its Electrochemical Performance in Lithium-ion Batteries. *Electrochim Acta*. 2010, vol. 55, 5006–5013.
- Liu S.Y., Xie J., Pan Q., Wu C.Y., Cao G.S., Zhu T., Zhao X.B. Graphene Anchored with Nanocrystal Fe<sub>2</sub>O<sub>3</sub> with Improved Electrochemical Li-storage Properties. *Int J Electrochemical Science*. 2012, vol. 7, 354–362.
- Huang X.H., Tu J.P., Zhang C.Q., Xiang J.Y. Net-structured NiO–C Nano Composite as Li-intercalation Electrode Material. *Electrochem Commun*. 2007, vol. 9, 1180–1184.
- Mi H., Xu Y., Shi W., Yoo H., Mo Oh S. Flocculant-assisted Synthesis of Fe<sub>2</sub>O<sub>3</sub>/carbon Composites for Superior Lithium Rechargeable Batteries. *Mater Res Bull*. 2012, vol. 47, 152–155.
- Li M.Y., Wang Y., Liu C.L., Gao H., Dong W.S. Iron Oxide/Carbon Microsphere Lithium-ion Battery Electrode with High Capacity and Good Cycling Stability. *Electrochim Acta*. 2012, vol. 67, 187–193.
- Rahman M.M., Chou S.L., Zhong C., Wang J.Z., Wexler D., Liu H.K. Spray Pyrolyzed NiO–C Nanocomposite as an Anode Material for the Lithium-ion Battery with Enhanced Capacity Retention. *Solid State Ionics*. 2012, vol. 180, 1646–1651.
- Legodi M.A., Waal D.D. The Preparation of Magnetite, Goethite, Hematite and Maghemite of Pigment Quality from Mill Scale Iron Waste. *Dyes Pigments*. 2007, vol. 74, 161–168.
- Qiao H., Xiao L., Zheng Z., Liu H., Jia F., Zhang L. One-pot Synthesis of CoO/C Hybrid Microspheres as Anode Materials for Lithium-ion Batteries. *J Power Sources*. 2008, vol. 185, 486–491.
- Zheng J., Liu Z.Q. One-step Solvothermal Synthesis of Fe<sub>3</sub>O<sub>4</sub>/C Core-shell Nanoparticles with Tunable Sizes. *Nanotechnology*. 2012, vol. 23, 165601.
- Wang L., Zhao Y., Lai Q., Hao Y. Preparation of 3D Rose-like NiO Complex Structure and its Electrochemical Property. *J Alloy Compd*. 2010, vol. 95, 82–87.

18. Wang Q., Li H., Chen L., Huang X. Novel Spherical Microporous Carbon as Anode Material for Li-ion Batteries. *Solid State Ionics*. 2002, vol. 152, 43–50.
19. Du H., Jiao L., Wang Q., Guo L., Wang Y., Yuan H. Facile Carbonaceous Microspheres Templated Synthesis of  $\text{Co}_3\text{O}_4$  Hollow Spheres and their Electrochemical Performances in Supercapacitors. *Nano Research*. 2013, vol. 6, 87–98.
20. Chen Y., Shi X., Han B., Qin H., Li Z., Lu Y. The Complete Control for the Nanosize of Spherical MCM-41. *JNN*. 2012, vol. 12, 1–11.

*Received 11.07.14*

*Accepted 21.10.14*

### Реферат

В этой работе рассматривается одноступенчатый способ изготовления микросфер  $\text{Fe}_2\text{O}_3/\text{C}$  с помощью

обкатки чешуек оксида при сольвотермическом синтезе. Термогравиметрический анализ (ТГА) проводили с целью определения количества углерода в синтезированных образцах. Только пики  $\text{Fe}_2\text{O}_3$  можно наблюдать на дифрактометрических рентгенограммах; углерод в композите был аморфным. Рассчитанное содержание углерода в композите было, примерно, 72 масс.%. После отжига при  $800^\circ\text{C}$ , сканирующая электронная микроскопия показала, что поверхность микросфер была довольно гладкой и их диаметры были в пределах 1–3,5 мкм. Исследование механизма формирования микросферы  $\text{Fe}_2\text{O}_3/\text{C}$  показало, что наночастицы  $\text{Fe}_2\text{O}_3$  однородно распределены в углеродной матрице.

*Ключевые слова: микросферы, сольвотермальный анализ,  $\text{Fe}_2\text{O}_3$ , углерод, электрод.*